ARTICLE

TRIM34 attenuates colon inflammation and tumorigenesis by sustaining barrier integrity

Qiaoshi Lian[1], Shanshan Yan[1,2], Qi Yin[1,3], Chenghua Yan[1], Wanwei Zheng[4], Wangpeng Gu[1,2], Xinhao Zhao[1], Weiguo Fan[1], Xuezhen Li[1], Liyan Ma[1], Zhiyang Ling[1], Yaguang Zhang[1], Jie Liu[4,5], Jinsong Li[3] and Bing Sun[1]

Loss of the colonic inner mucus layer leads to spontaneously severe colitis and colorectal cancer. However, key host factors that may control the generation of the inner mucus layer are rarely reported. Here, we identify a novel function of TRIM34 in goblet cells (GCs) in controlling inner mucus layer generation. Upon DSS treatment, TRIM34 deficiency led to a reduction in Muc2 secretion by GCs and subsequent defects in the inner mucus layer. This outcome rendered TRIM34-deficient mice more susceptible to DSS-induced colitis and colitis-associated colorectal cancer. Mechanistic experiments demonstrated that TRIM34 controlled TLR signaling-induced Nox/Duox-dependent ROS synthesis, thereby promoting the compound exocytosis of Muc2 by colonic GCs that were exposed to bacterial TLR ligands. Clinical analysis revealed that TRIM34 levels in patient samples were correlated with the outcome of ulcerative colitis (UC) and the prognosis of rectal adenocarcinoma. This study indicates that TRIM34 expression in GCs plays an essential role in generating the inner mucus layer and preventing excessive colon inflammation and tumorigenesis.

Keywords: Colon inflammation; Goblet cell; Toll-like receptor; TRIM34; Muc2

Cellular & Molecular Immunology (2021) 18:350–362; https://doi.org/10.1038/s41423-020-0366-2

INTRODUCTION

Inflammation is generally considered a protective host response against pathogen infection and tissue damage.[1] However, uncontrolled inflammation is harmful to host health. Inflammatory bowel disease (IBD) comprises typical inflammation-related disorders of the gastrointestinal tract. The incidence of IBD is increasing worldwide.[2–5] The two main types of IBD are UC and Crohn's disease (CD), which are distinguished by inflammatory site and the nature of the inflammatory pathology. There is no effective treatment for either condition.[6,7] Long-term chronic inflammation is a critical risk factor for tumorigenesis,[8] and patients with IBD have a higher risk of developing CAC,[9–11] one of the leading causes of cancer-related deaths.[12] However, the precise molecular mechanisms of IBD pathogenesis and IBD-related colorectal tumor formation remain incompletely understood.

Accumulating evidence suggests that IBD results from an aberrant immune response that is initiated by inappropriate interactions between the host cell and the intestinal microbiota,[13–15] especially in UC, which is largely associated with commensal bacteria.[16–18] The intestinal mucosal surface is largely colonized by microbiota consisting of bacteria, fungi, parasites, and viruses, most of which inhabit the distal intestine.[19] In a steady state, the colonic microbiota is separated from the mucosa by an overlying mucus layer, which prevents physical contact between microbes and epithelial cells. Colonic mucus layers are composed of inner and outer layers.[20] The inner mucus layer is impenetrable to bacteria, whereas the outer layer serves as a habitat for commensal bacteria.[20,21] Hence, the inner mucus layer is indispensable for the host as a physical separation between the commensal bacteria and colonic mucosa to prevent uncontrolled colon inflammation in the host. Muc2 is a gel-forming mucin and is the major component of colonic mucus. Loss of Muc2 leads to defects in the inner mucus layer and direct contact between bacteria and epithelial cells, which result in the activation of the immune system and inflammation.[20,22] Muc2-deficient mice spontaneously develop severe colitis and eventually colorectal cancer.[23,24] In addition, patients with active UC and some patients in remission from colitis present with dysfunction of the mucus, in which the inner layer is thinner and can be penetrated by bacteria.[25] Thus, inner mucus formation must be tightly controlled to avoid colonic inflammation-associated diseases.

Colonic GCs are responsible for synthesizing and secreting gel-forming mucins, especially Muc2. GCs are located throughout the whole colonic crypt, including the upper and lower crypts. Before Muc2 is released into the lumen, it is stored in GC granules.[21] Muc2 is generally released via one of two mechanisms: vesicle fusion-mediated basal secretion and compound exocytosis-

[1]State Key Laboratory of Cell Biology, CAS Center for Excellence in Molecular Cell Science, Shanghai Institute of Biochemistry and Cell Biology, Chinese Academy of Sciences, University of Chinese Academy of Sciences, 320 Yueyang Road, Shanghai 200031, China; [2]School of Life Sciences, University of Science and Technology of China, Hefei 230022, China; [3]State Key Laboratory of Cell Biology, Shanghai Key Laboratory of Molecular Andrology, CAS Center for Excellence in Molecular Cell Science, Shanghai institute of Biochemistry and Cell Biology, Chinese Academy of Sciences, University of Chinese Academy of Sciences, 320 Yueyang Road, Shanghai 200031, China; [4]Department of Digestive Diseases, Huashan Hospital, Fudan University, 12 Middle Wulumuqi Road, Shanghai 200040, China and [5]Institutes of Biomedical Sciences and Department of Immunology, Shanghai Medical School, Fudan University, 138 Yi Xue Yuan Road, Shanghai 200032, China
Correspondence: Yaguang Zhang (zhangyaguang@sibcb.ac.cn) or Jie Liu (jieliu@fudan.edu.cn) or Jinsong Li (jsli@sibcb.ac.cn) or Bing Sun (bsun@sibs.ac.cn)
These authors contributed equally: Qiaoshi Lian, Shanshan Yan, Qi Yin, Chenghua Yan

Received: 3 August 2019 Accepted: 19 January 2020
Published online: 24 February 2020

mediated stimulated secretion in response to external stimuli.[18,22,26,27] Compound exocytosis is reported to be mediated by endocytosis, autophagy, and inflammasome assembly and activation.[28,29] However, little is known about the regulatory mechanism by which Muc2 is released through compound exocytosis.

The tripartite motif-containing protein (TRIM) family is frequently implicated in the modulation of the inflammatory response and host defense.[30,31] In our laboratory, we have discovered the regulatory roles of TRIM30α, TRIM44, and TRIM35 in various inflammation and interferon response-mediated signaling pathways.[32–35] In this study, we identified an important role of TRIM34 in regulating intestinal inflammation by controlling the exocytosis of Muc2 from colonic GCs. The function of TRIM34 is crucial for forming the inner mucus layer, protecting the colonic mucosa from excessive inflammation in a DSS-induced colitis model. The results provide a novel mechanism that explains how host factors control the pathogenesis of commensal bacteria-related colitis and inflammation-driven colorectal cancer.

MATERIALS AND METHODS

Patients

Colonic mucosal samples were collected from UC patients and healthy subjects during endoscopy at the Department of Digestive Diseases, Huashan Hospital, Fudan University.

Mice

TRIM34- and TRIM35-deficient mice were generated on a C57BL/6 background using CRISPR/Cas9 technology. A TRIM34-deficient mouse strain was designed by inserting an additional base T into the first exon of both *Trim34a* and *Trim34b*. A TRIM35-deficient mouse strain was designed by inserting the additional base GAATTCG into the first exon of the *Trim35* gene. TRIM34- and TRIM35-deficient mice were identified by polymerase chain reaction (PCR) amplification and DNA sequencing with primers 5′-AATCTGCCTAGCCATCCA-3′ and 5′-TGAGAACGCTCACAAACCCA-3′ and primers 5′-CTCCCAGATCTTCAGCAGGG-3′ and 5′-GGTTGTTGAGCGTGTGGTTG-3′, respectively. Mice were bred and housed under specific pathogen-free conditions. Age- (6–12 weeks) and sex-matched mice were used. All animal experiments were performed in accordance with the NIH Guide for the Care and Use of Laboratory Animals.

Induction of experimental colitis and CAC

To induce acute colitis, mice were administered 2.5–4% dextran sulfate sodium salt (DSS) (MW 36–50 kDa; MP Biomedical) dissolved in drinking water for five consecutive days as previously described.[36] In some special experiments, the mice were administered DSS for fewer than five days and then sacrificed according to the indicated requirements. Clinical stool consistency and rectal bleeding were scored on days 5 and 6 as previously described.[36]

To induce colitis-associated cancer (CAC) (Fig. 8a), the mice were injected intraperitoneally once with azoxymethane (AOM) (10 mg/kg body weight, Sigma) and treated with three cycles of 2.5% DSS in drinking water for five days, followed by normal drinking water, as previously described.[37]

For induction of $CD4^+$ T cell-mediated colitis, naïve $CD4^+$ T cells from wild-type and TRIM34-deficient mice were purified by negative selection using a MACS isolation kit (stem cell) and intraperitoneally injected into $Rag1^{-/-}$ mice (8–10 weeks) with 5×10^5 cells per mouse as previously described.[38] The mice were weighed on the indicated days and sacrificed at 8 weeks after T-cell transfer.

Histological analysis and macroscopic polyp assessment

For the macroscopic polyp analysis, entire colons were removed, flushed with phosphate-buffered saline and longitudinally opened to examine macroscopic polyp formation, as previously described.[37] Tumor loads were determined by adding the diameters of all whole colon tumors per mouse.[37]

For the histopathological analysis, the colons were fixed in 4% paraformaldehyde and stained with H&E. The pathology of the sections was scored blindly based on the extent and severity of the inflammation, ulceration, and hyperplasia of the mucosa, as previously described.[39]

To analyze goblet cells (GCs) and mucus layer preservation ex vivo, colons containing stool pellets were submerged in methanol-Carnoy's fixative.[40] The fixed colons were then stained using Alcian blue and periodic acid-Schiff (AB/PAS). The thickness of the inner mucus was measured perpendicular to the mucosal surface from the edge of the epithelium to the outermost part of the mucus layer. Four to five measurements were taken per slide for every 50 μm along the length of the specimen from an arbitrary starting point. Approximately, five slides per mouse were measured and the mean was calculated.[41]

Immunostaining and fluorescence in situ hybridization

Freshly isolated mouse colons or colon explants were treated with lipopolysaccharide (LPS) (Sigma, 200 or 500 μg/ml) or P3CSK4 (Invivogen, 100 μg/ml) for 45 min, fixed in methanol-Carnoy's fixative and then embedded in paraffin and cut into 5- to 8-μm-thick sections. Immunostaining was performed using a primary antibody for Muc2 (H-300, Santa Cruz) followed by incubation with a Cy3-conjugated secondary antibody or FITC-conjugated UEA-1 lectin (Sigma, 2.5 μg/ml). To detect all bacteria, the sections were incubated with 1 μg of a Cy3-conjugated EUB338 DNA probe (5′-GCTGCCTCCCGTAGGAGT-3′) and then processed. Human colon mucosa samples obtained from healthy donors were stained using primary antibodies for Muc2 (F2, Santa Cruz) and TRIM34 (Abcam, ab180130) and then incubated with FITC-conjugated and Cy3-conjugated secondary antibodies. DAPI (4′, 6′-diamidino-2-phenylindole) was used to stain the nuclei.

Generation of radiated bone marrow chimeras

Bone marrow-chimera mice were generated as previously described.[42] Briefly, 8- to 10-week-old wild-type and TRIM34-deficient mice were exposed to a lethal dose of irradiation (8.5 Gy), and these mice were then used as the recipient mice. Bone marrow cells isolated from 8- to 10-week-old wild-type and TRIM34-deficient donor mice were intravenously injected into the recipient mice at a dose of 1×10^7 cells per mouse 12 h post irradiation. After 8 weeks of reconstitution, the mice were administered 4% DSS to induce acute colitis (Fig. 2a). The efficiency of the bone marrow reconstitution was validated using DNA sequencing of samples taken from tails and blood leukocytes.

Isolation of colonic epithelial cells and ex vivo ROS quantification

Colon tissues were freshly isolated, longitudinally opened and washed with sterile Hanks' balanced salt solution (HBSS) five times. The colons were then cut into pieces smaller than 5 mm in length and washed with HBSS three times. They were then incubated in HBSS containing 5 mM ethylenediaminetetraacetic acid, 5% fetal calf serum (v/v) and 1 mM DTT at 37 °C in a 200 rpm shaking incubator for 30 min.[40] The HBSS did not contain Ca^{2+} or Mg^{2+}. The tissues were vortexed for 1 min to disassociate the cells, and the suspended cells were subsequently passed through a 40 μm filter (Corning). The isolated cells were used for RNA extraction or were counted and placed into a 24-well plate that was precoated with collagen I (Invitrogen). After the cells were cultured for 4–6 h, they were labeled with reactive oxygen species (ROS)-sensitive DCFDA-AM dye (10 μM, Sigma) and then stimulated with Toll-like receptors (TLR) ligands, including LPS obtained from *Escherichia coli* (Sigma, 200 μg/ml) or P3CSK4 (Invivogen, 100 μg/ml), for 30–60 min at 37 °C. ROS production was quantified by measuring DCFDA fluorescence (494–520 nm) using a plate reader (BioTek).

Antibiotic treatment

To treat the animals with antibiotics, age- and sex-matched wild-type and TRIM34-deficient mice were treated with a cocktail of antibiotics, including ampicillin sodium salt (1 g/l), metronidazole (1 g/l), vancomycin hydrochloride (0.5 g/l), and neomycin (1 g/l) (all introduced in drinking water) for 18–20 days, as previously described.[42]

Scanning and transmission electron microscopy

Murine distal colon tissues (0.5 cm^2) were freshly isolated and fixed in 150 mM cacodylate buffer containing 2.5% glutaraldehyde overnight at 4 °C. The fixed tissues were washed three times with sodium cacodylate buffer and incubated in 1% osmium tetroxide for 1–1.5 h. The samples were then washed three times with sodium cacodylate buffer and further dehydrated through an ethanol series. For scanning electron microscopy (SEM), the samples were all viewed using an FEI Quanta transmission electron microscopy (TEM) at 20 kV. For TEM, the samples were further submerged in Epon812 resin and incubated overnight at 60 °C. Ultrathin sections were cut using an EM UC6 ultramicrotome (Leica). Sections (70 nm thick) were stained with 2% uranyl acetate for 10 min and then 1% lead citrate for 5 min.

Quantitative RT-PCR analysis

Total RNA was extracted from cells or tissues using TRIzol reagent (Invitrogen) according to the manufacturer's instructions. RNA was reverse-transcribed into cDNA using a PrimeScript RT kit (TaKaRa). Q-PCR was performed using SYBR Green PCR Master Mix (Toyobo) on an Applied Biosystems QuantStudioTM 6 Flex detection system. HPRT and GAPDH were used as housekeeping gene controls for the mouse samples and human samples, respectively. The following primers were used to amplify the major targeting genes:

Human TRIM34 FW: 5′-CCGAGGTTTTGACTCTCTCCAT-3′;
Human TRIM34 RV: 5′-GCCTGCTTCATAGTCGAGGAA-3′;
Human GAPDH FW: 5′-CCAGGTGGTCTCCTCTGACTTC-3′;
Human GAPDH RV: 5′-GTGGTCGTTGAGGGCAATG-3′;
TRIM34 FW: 5′-CAACCATGGATCACTCATTTACAAG-3′;
TRIM34 RV: 5′-CCCAAGGATTGAAGTATGGATAGG-3′;
Muc2 FW: 5′-ATGCCCACCTCCTCAAAGAC-3′;
Muc2 RV: 5′-GTAGTTTCCGTTGGAACAGTGAA-3′;
Atoh1 FW 5′-AAAGGAGGCTGGCAGCAA-3′;
Atoh1 RV 5′-TGGTTCAGCCCGTGCAT-3′;
Gfi1 FW 5′-TTTTGGAGGCCCCCTTCT-3′;
Gfi1 RV 5′-AGAGAGCGGCACAGTGACTTC-3′;
Hes1 FW 5′-CCCCAGCCAGTGTCAACAC-3′;
Hes1 RV 5′-TGTGCTCAGAGGCCGTCTT-3′;
Klf4 FW 5′-AGGCACACCTGCGAACTCA-3′;
Klf4 RV 5′-CAGCCGTCCCAGTCACAGT-3′;
Spdef FW 5′-GCAGGTGCAATCGATGGTT-3′;
Spdef RV 5′-TGCAGGCCGTCTCAATATCTT-3′;
TNF FW: 5′-AAGCCTGTAGCCCACGTCGTA-3′;
TNF RV: 5′-GGCACCACTAGTTGGTTGTCTTTG-3′;
HPRT FW: 5′-TGCTCGAGATGTCATGAAGGAG-3′; and
HPRT RV: 5′-CAGAGGGCCACAATGTGATG-3′.

Ethics Statement

All animal experiments were approved by the Institutional Animal Care and Use Committee of the Shanghai Institute of Biochemistry and Cell Biology, Chinese Academy of Sciences (Approval number IBCBSPF0028). All animal experiments were performed in accordance with the NIH Guide for the Care and Use of Laboratory Animals.

The use of patient samples was approved by the Department of Digestive Diseases, Huashan Hospital, Fudan University (Ethics approval 2013-005-V1). The patients and healthy donors provided written informed consent.

Statistical analysis

Data are presented as the mean ± SEM. P values < 0.05 were considered significant. Significant differences were analyzed using Student's t test and one-way or two-way analysis of variance, as indicated. Kaplan–Meier survival curves were assessed using log-rank (Mantel–Cox) tests.

RESULTS

Generation of TRIM34-deficient and TRIM35-deficient mice

Based on our previous studies and extensive research on the roles of TRIM family members in regulating inflammation and host defense against pathogens,[30,32,33] we speculated that TRIM family members are also involved in inflammation triggered by microbes in the intestinal tract. We generated TRIM34- and TRIM35-deficient mouse strains using CRISPR/Cas9 technology (Supplementary Fig. 1a–c). Because 475 of the 485 total amino acids in murine TRIM34a and TRIM34b have shared identity, a specific sgRNA was designed to target both *Trim34a* and *Trim34b* for insert mutations, which were validated by DNA sequencing (Supplementary Fig. 1d).

TRIM34-deficient mice develop severe DSS-induced colitis

To assess the regulatory role of TRIM34 and TRIM35 in intestinal inflammation, a dextran sodium sulfate (DSS)-induced colitis model was utilized. Upon DSS administration, TRIM34-deficient mice showed greater weight loss and morbidity than were shown by the wild-type mice, whereas there was no clear difference between the TRIM35-deficient mice and wild-type controls (Fig. 1a, b). On day 8, most wild-type mice began to recover, while all the TRIM34-deficient mice died in the acute phase of the disease. The increased severity of the colitis observed in the TRIM34-deficient mice manifested as greater diarrhea and bloody stools (Fig. 1c), shorter colon length (Fig. 1d, e), and increased clinical scores (Fig. 1f). To further evaluate this hyperinflammatory phenotype, histopathological sections of the colon were analyzed. Consistent with the clinical features described above, TRIM34-deficient mice displayed markedly increased inflammatory cell infiltration, significantly more ulceration and more structural damage (Fig. 1g, h). Notably, in the steady state without DSS treatment, the levels of the major three inflammatory cytokines (TNF-α, IL-6, and IL-17a) and colonic histopathology were similar between the TRIM34-deficient mice and wild-type mice (Supplementary Fig. 2). Collectively, these results demonstrate that TRIM34 deficiency promotes DSS-induced colon inflammation.

The nonhematopoietic compartment plays a determining role in severe colitis in the TRIM34-deficient mice

It was very important to identify which cell types determine the severe inflammation in the TRIM34-deficient mice; therefore, we carried out two experiments. Since Th1 and Th17 cells are key cells that initiate the inflammatory response during IBD progression,[13] we first wondered whether $CD4^+$ T cells played a role in colitis susceptibility in the TRIM34-deficient mice. To address this question, naïve $CD4^+$ T-mediated colitis in *Rag1*$^{-/-}$ mice was tested.[38] The results showed that there was no significant difference in colitis severity between the *Rag1*$^{-/-}$ mice receiving wild-type $CD4^+$ T cells and those receiving TRIM34-deficient $CD4^+$ T cells, as reflected by the results from the survival, body weight, ratio of colon weight/length and histopathological analyses (Supplementary Fig. 3). These data ruled out the contribution of TRIM34 in $CD4^+$ T cells.

Next, bone marrow-chimera mice were generated to evaluate the contribution of TRIM34 from hematopoietic and nonhematopoietic cells. Whole body-irradiated wild-type and TRIM34-deficient recipient mice were reconstituted with either wild-type or TRIM34-deficient bone marrow and then challenged with DSS (Fig. 2a). The results revealed that the TRIM34-deficient recipient mice were substantially more sensitive than the wild-type recipient mice to

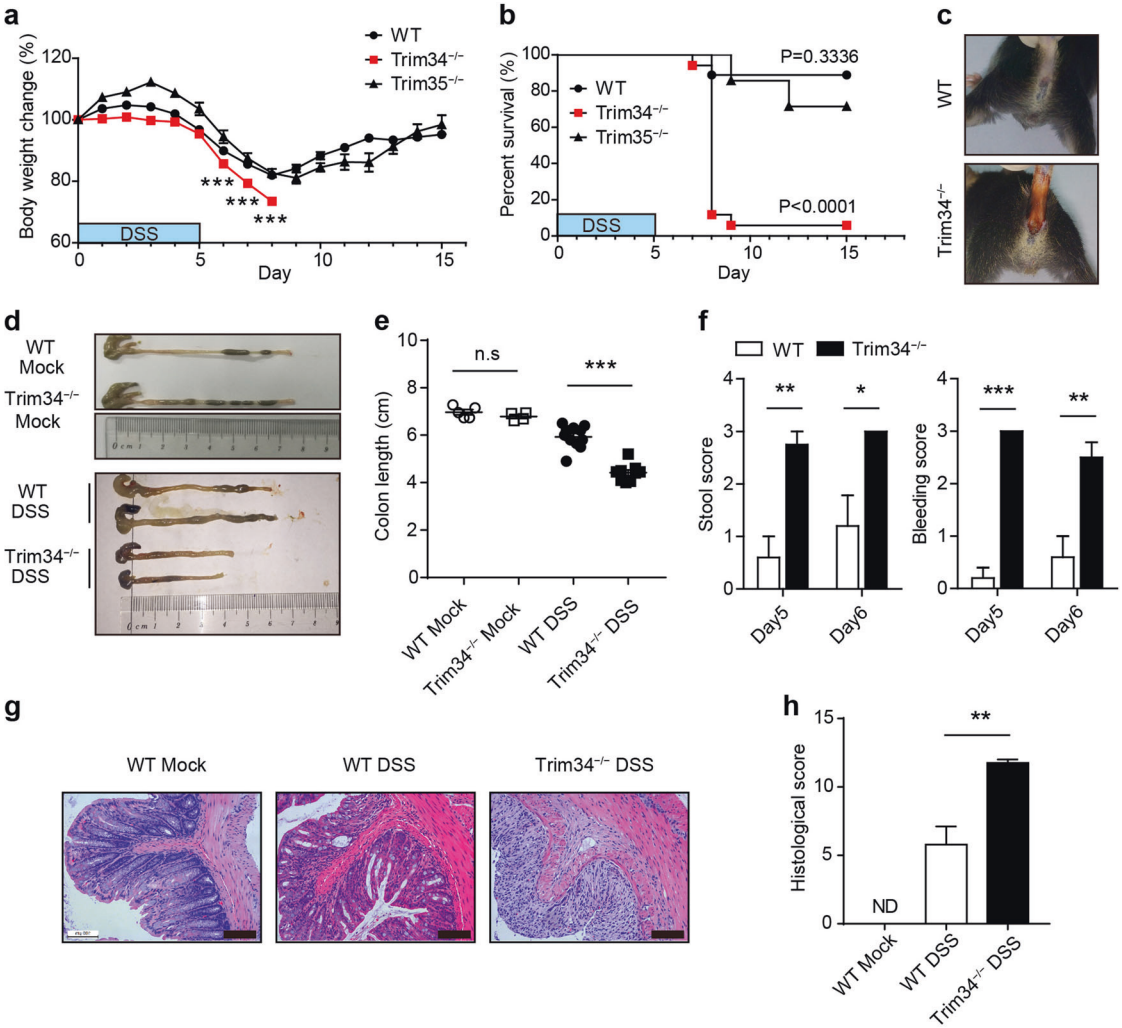

Fig. 1 TRIM34 is required to prevent DSS-induced colitis. **a**, **b** Wild-type ($n = 7$), TRIM34-deficient ($n = 7$), and TRIM35-deficient ($n = 7$) mice were treated with 3% DSS as indicated and monitored daily for changes in body weight (**a**) and survival (**b**) until the end of the experiment. **c**–**e** Wild-type ($n = 11$) and TRIM34-deficient ($n = 9$) mice were treated with 3% DSS for 5 days. Wild-type mice without DSS challenge ($n = 5$) and TRIM34-deficient mice without DSS challenge ($n = 4$) served as controls. **c** Representative images of diarrhea/bloody stools observed on day 5. **d**, **e** Colon length on day 7. **f**–**h** Wild-type and TRIM34-deficient mice were treated with 2.5% DSS for 5 days (WT, $n = 5$; KO, $n = 4$). Untreated wild-type mice served as controls ($n = 3$). **f** Clinical stool and bleeding scores were determined on both day 5 and day 6. **g** Representative images of pathological H&E-stained colon sections collected on day 7. Scale bar, 100 μm. **h** Histopathological scores for (**g**). The data shown are representative of three independent experiments and depict the means ± SEM; $^{*}P < 0.05$, $^{**}P < 0.01$, and $^{***}P < 0.001$; ND not detected; **a**, **e**, **f**, **h**, unpaired Student's *t* test; **b** log-rank test

DSS-induced colitis, regardless of whether the donor cells were obtained from wild-type or TRIM34-deficient mice, as shown by visible diarrhea and bloody stools (Fig. 2b), shortened colon length (Fig. 2c, d), and higher clinical scores (Fig. 2e, f). In contrast, there was no significant difference between the wild-type recipient mice that were reconstituted with bone marrow cells derived from the wild-type or TRIM34-deficient mice (Fig. 2b–f). The increase in the severity observed in the TRIM34-deficient recipient mice was further confirmed in a histopathological analysis of colon sections (Fig. 2g, h). Together, these results indicate that TRIM34 expression in the nonhematopoietic component is essential for preventing excessive inflammation induced by DSS.

The integrity of the inner mucus layer is impaired in the TRIM34-deficient mice following DSS challenge

Next, we sought to determine how TRIM34 expression by nonhematopoietic cells modulated the pathogenesis of DSS-induced colitis. Because TRIM34-deficient mice were more sensitive to DSS-induced colitis in the early acute phase than were the wild-type mice (Fig. 1), we first examined whether TRIM34 regulates colonic barrier integrity, which is primarily generated by colonic epithelial cells. In the colon, the inner mucus layer is well known as the primary physical barrier that provides separation from microbes in order to avoid excessive inflammation. Hence, the inner mucus layer was examined in the early phase after mouse treatment with DSS. The results revealed that, in a steady state, TRIM34-deficient mice harbored an intact inner mucus layer similar to that of the wild-type mice. By day 3 and day 4 following mouse exposure to DSS, the inner mucus layer was indeed impaired and exhibited decreased thickness. Strikingly, in contrast to that of the wild-type mice, the inner mucus layer in the TRIM34-deficient mice was extensively damaged by treatment with DSS, which also resulted in the near-complete disappearance of the inner mucus layer by day 3 or day 4 (Fig. 3a, b and Supplementary Fig. 4a), indicating that the generation of the inner mucus layer was defective in the TRIM34-deficient mice. To further verify that the inner mucus layer was defective, we used SEM to visualize the mucosal surface. The SEM results revealed that, in the

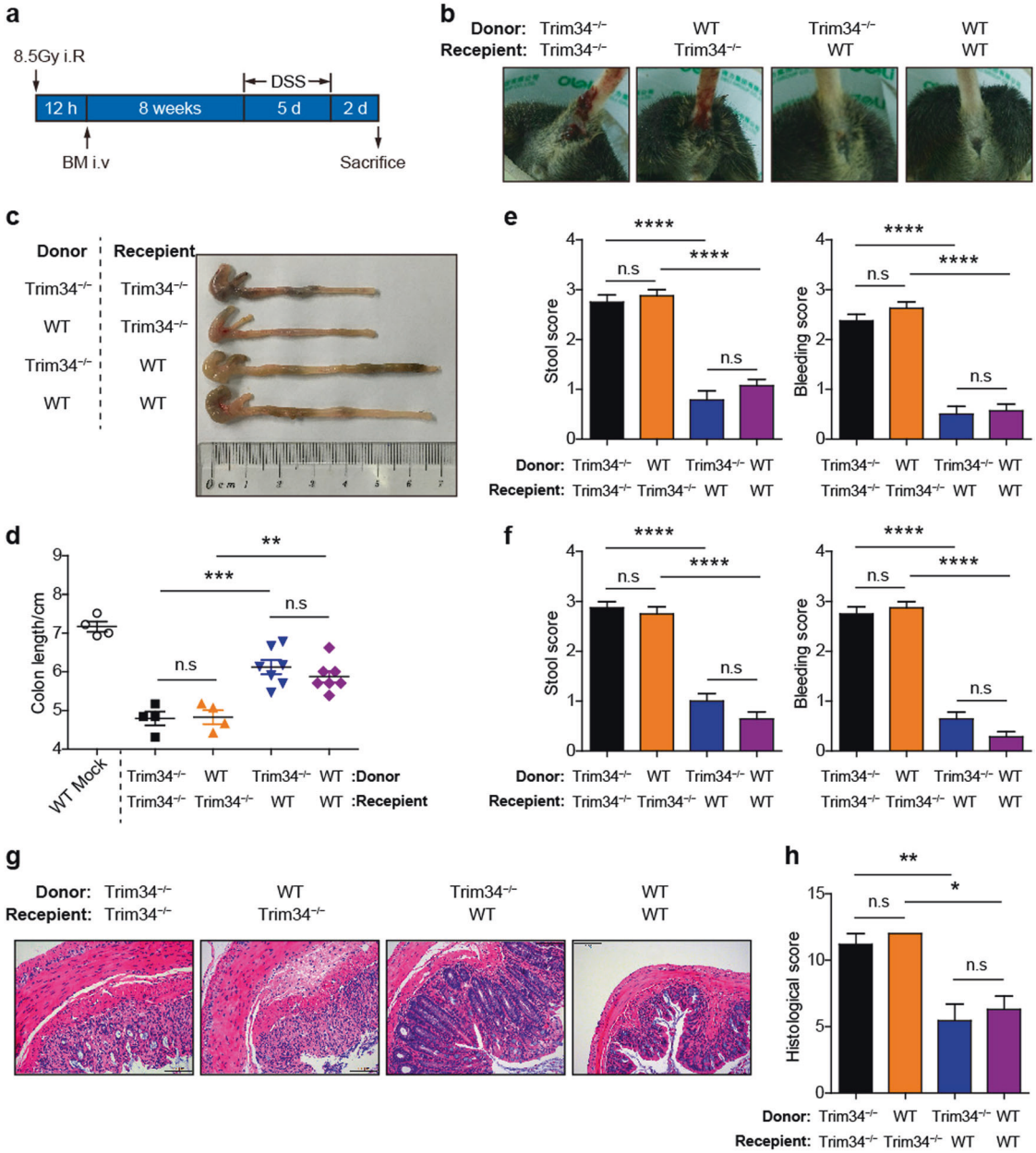

Fig. 2 Nonhematopoietic TRIM34 is responsible for protecting against acute colitis. Chimeric mice were generated by transplanting bone marrow cells from donor mice into lethally irradiated recipient mice (donor mice > recipient mice: WT > WT, $n = 7$; KO > WT, $n = 7$; WT > KO, $n = 4$; KO > KO, $n = 4$). After 8 weeks of reconstitution, the four groups of mice were treated with 4% DSS for 5 days. **a** Flow chart of the generation and induction processes. **b** Representative images of diarrhea and bloody stools on day 5 post-DSS challenge. **c** Images of the colons from the mice sacrificed on day 7. **d** Colon length in (**c**). **e**, **f** Stool and bleeding scores on day 5 (**e**) and day 6 (**f**). **g** Representative images of H&E-stained colon sections. Scale bar, 100 μm. **h** Histopathological scores of (**g**). The data shown are representative of three independent experiments and depict the means ± SEM; $^{*}P < 0.05$, $^{**}P < 0.01$, and $^{***}P < 0.001$, $^{****}P < 0.0001$; n.s. not significant. **d**–**f**, **h** One-way ANOVA (Tukey's multiple-comparisons test)

TRIM34-deficient mice, the colon exhibited a mucosal surface similar to that of the wild-type mice that were not treated with DSS, whereas exposure to DSS led to a markedly damaged mucosal surface and larger visible protruding mucin granules in the TRIM34-deficient mice (Fig. 3c).

As Muc2 is the primary component of the inner mucus layer, we then examined the integrity of the Muc2-expressing layer in the TRIM34-deficient mice. The immunofluorescence data showed that, following treatment with DSS for 3 days, the integrity of the Muc2-expressing layer was more severely damaged in the TRIM34-deficient mice than it was in the wild-type mice (Fig. 3d, right). In contrast, in the mice not exposed to DSS, the Muc2-expressing layer was similarly unchanged in the wild-type and TRIM34-deficient mice (Fig. 3d, left). The formation of the Muc2-expressing layer is dependent on the synthesis, maturation and secretion of Muc2. The Muc2 level was comparable between TRIM34-deficient and wild-type mice (Fig. 3d and Supplementary Fig. 4b), excluding the possibility of dysfunction in Muc2 synthesis. Of note, we did not observe any significant differences in the expression levels of other mucus components between the wild-type and TRIM34-

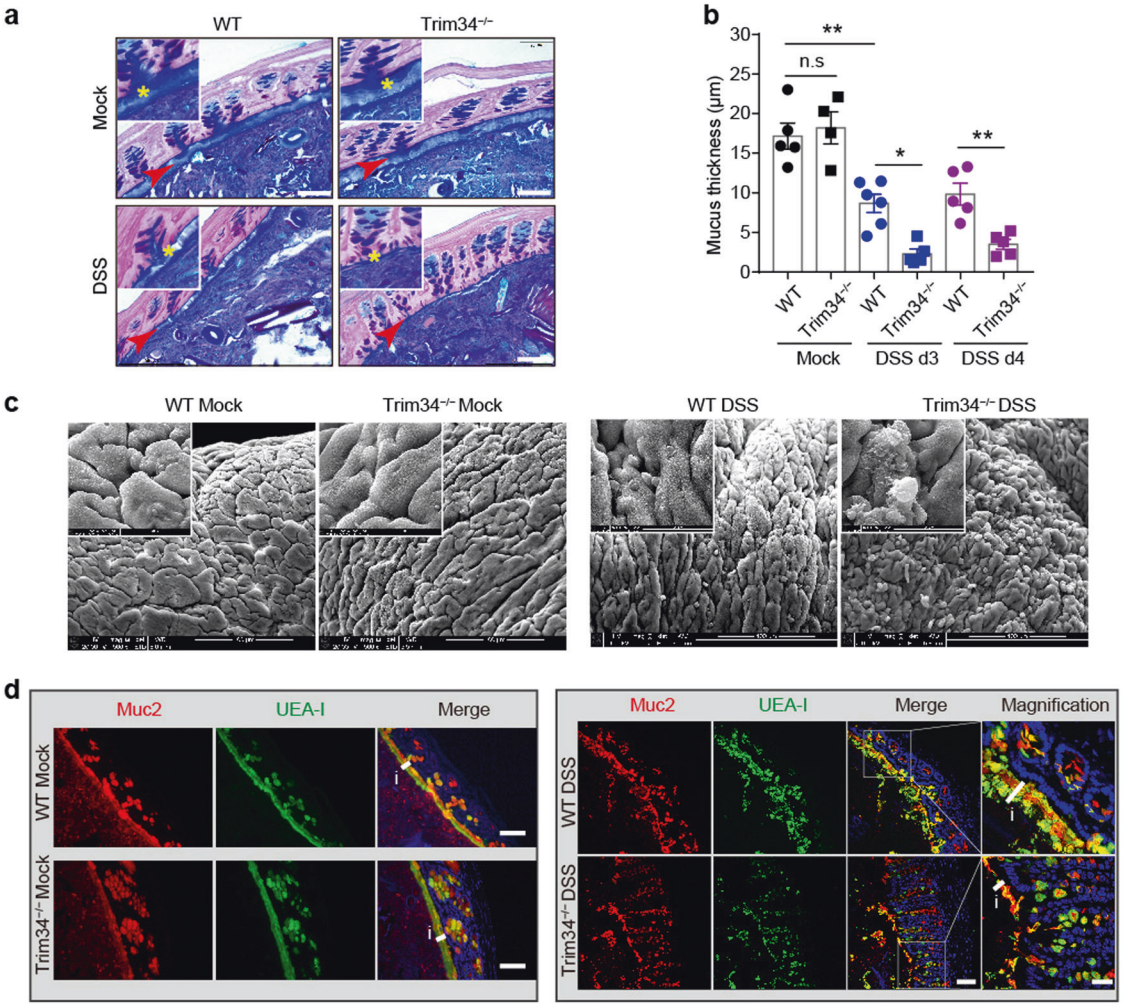

Fig. 3 TRIM34 is important for preserving inner mucus layer integrity following challenge with DSS. **a** Representative images of AB/PAS-stained colonic sections containing stool pellets from mice treated with 3% DSS for 3 days or from untreated mice. Untreated WT ($n = 5$) and KO ($n = 4$), DSS-treated WT ($n = 6$), and KO ($n = 5$) mice. Asterisks and arrows highlight the inner mucus layers. Scale bar, 50 μm. **b** Measurement of mucus thickness on day 3 and day 4. **c** Images obtained by scanning electron microscopy of colons from untreated mice and mice treated with 3% DSS for 3 days. Scale bar, 100 μm. **d** Colon sections stained for Muc2 (red), fucose (UEA-1, green), and nuclei (DAPI, blue) from untreated mice or mice treated with 3% DSS for 3 days. Scale bar, 50 μm, except for the magnified image, in which the scale bar is 20 μm. The letter i and short line highlight the inner mucus layers. The data shown are representative of two (**c**) or three (**a**, **b**, **d**) independent experiments and depict the means ± SEM; *$P < 0.05$ and **$P < 0.01$; n.s, not significant. **b** One-way ANOVA (Tukey's multiple-comparisons test)

deficient mice, including Muc1, CLCA1, Arg1, and Zg16 (Supplementary Fig. 4c). Next, colon sections were stained for Muc2 and fucosylated glycoproteins using *Ulex europaeus* agglutinin-1 (UEA-1) lectin. We detected the colocalization of Muc2 and UEA-1 in colonic mucosae from the mice treated with DSS and untreated controls. The immunofluorescence images and results from the quantitative colocalization rate analysis showed that, regardless of whether the mice were treated with DSS, Muc2 labeling was highly correlated with UEA-1 labeling in both the TRIM34-deficient and wild-type mice (Fig. 3d and Supplementary Fig. 4d). These results indicate that Muc2 matures normally, ruling out the possibility of a dysfunction in Muc2 maturation. Notably, the TRIM34-deficient mice had a functional mucus structure compared to that of the wild-type controls (Supplementary Fig. 5a), which showed permeability comparable to that of the wild-type mice (Supplementary Fig. 5b). Collectively, based on the above results, we hypothesized that the defect in the inner mucus layer observed in the TRIM34-deficient mice might be caused by a dysfunction in Muc2 secretion following DSS challenge.

The exocytosis of Muc2 from GCs is attenuated in the TRIM34-deficient mice

The inner mucus layer is mainly produced by colonic GCs, which are a specialized cell located in the epithelium. Muc2 and other mucins are all synthesized, processed and secreted by GCs. Before they are secreted into the lumen, Muc2, and other mucins are tightly packed into the granules of GCs.[21] Hence, we sought to determine whether TRIM34 regulates the secretion of mucin granules from GCs. To make this determination, we initially examined whether TRIM34 is expressed in GCs. Using flow cytometry (Supplementary Fig. 6), we sorted upper-crypt GCs ($CLCA1^+$ GCs), lower-crypt GCs ($CD24^{hi}$ GCs), and $CLCA1^-$ IECs that were freshly isolated, according to reported strategies.[43,44] The sorting efficiency was confirmed by the expression levels of Clca1 and Gfi1, specific transcriptional factors in GCs (Fig. 4a). The data showed that TRIM34 was expressed differentially: $CLCA1^+$ GCs > $CD24^{hi}$ GCs > $CLCA1^-$ IECs, indicating that TRIM34 is indeed expressed in GCs, particularly upper-crypt GCs in the epithelial compartment.

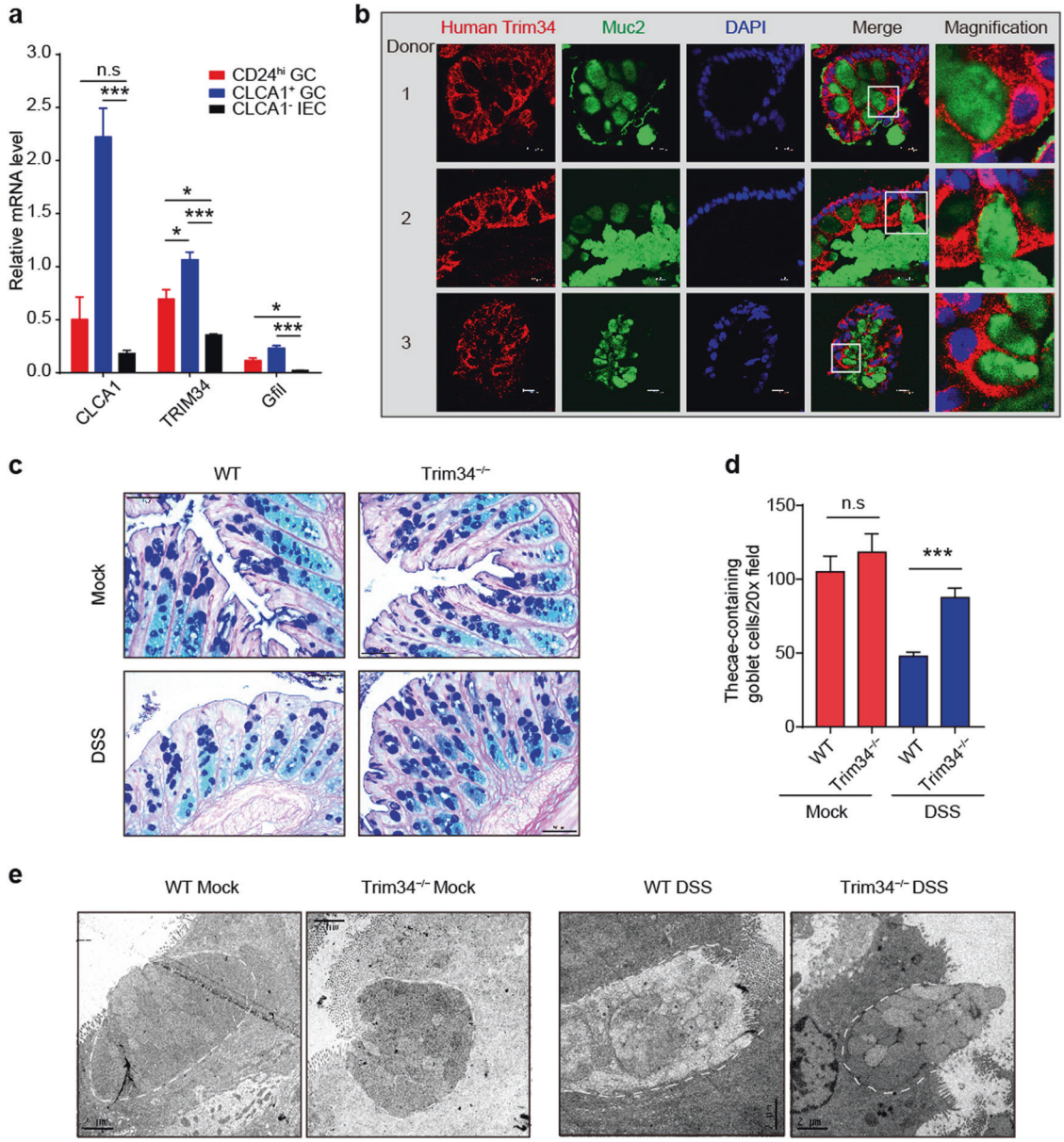

Fig. 4 TRIM34 deficiency attenuates the exocytosis of Muc2-containing granules from goblet cells following treatment with DSS. **a** Quantitative PCR analysis of CLCA1^{+} GCs, CD24^{hi} GCs, and CLCA1^{-} IECs. **b** Human colonic sections obtained from healthy donors were stained for TRIM34 (red), Muc2 (green) and nuclei (DAPI, blue). Scale bar, 10 μm. **c** Representative images of AB/PAS-stained colonic sections obtained from mice treated with 3% DSS for 3 days or untreated mice. Untreated WT ($n = 4$) and KO ($n = 3$), DSS-treated WT ($n = 5$) and KO ($n = 4$). Scale bar, 50 μm. **d** The number of thecae-containing goblet cells shown in (**c**). **e** Transmission electron microscopy of colons obtained from untreated mice or mice treated with 3% DSS for 3 days. Scale bar, 2 μm. The discontinuous white line highlights the edge of goblet cells. The data shown are representative of two (**e**) or three (**a**–**d**) independent experiments and depict the means ± SEM. *$P < 0.05$, **$P < 0.01$, ***$P < 0.001$. n.s. not significant. **a**, **d**, One-way ANOVA (Tukey's multiple-comparisons test)

To further validate the expression of TRIM34 in GCs, TRIM34 was labeled using immunofluorescence in human colonic mucosae. We then co-stained for TRIM34 and Muc2 and observed that in the colonic tissues from multiple human donors, TRIM34 was expressed in the area surrounding the theca that housed the mucin-containing granules in GCs labeled with Muc2 (Fig. 4b). These results demonstrate that TRIM34 is highly expressed by GCs.

Next, we stained the mucin granules located in the GCs of the colonic crypts. The results showed that the levels of mucin granule-containing GCs were comparable in the TRIM34-deficient and wild-type mice in the steady state. However, following exposure to DSS, the TRIM34-deficient mice had markedly higher numbers of granule-containing GCs in the crypts than were observed in wild-type mice (Fig. 4c, d). Interestingly, the mRNA levels of key transcription factors, namely, Atoh1, Hes1, Spdef, Klf4, and Gfi1, were similar in the TRIM34-deficient and wild-type mice, regardless of whether they were treated with DSS (Supplementary Fig. 7), ruling out the possibility of a difference in GC differentiation or maturation between these lines of mice. These data suggest that Muc2 secretion was impaired in TRIM34-deficient mice.

Finally, we used TEM to visualize the GCs in the theca. The TEM images showed that, at a steady state and at the apical surface of the theca, the GCs were filled with a normal number of mucin granules in both the TRIM34-deficient and control mice. Upon exposure to DSS, apical GCs were absent in the theca of the wild-type mice. Furthermore, the release of mucin granules from the

TRIM34-deficient GCs in the apical theca was greatly attenuated (Fig. 4e). Collectively, these findings indicate that TRIM34 modulates the exocytosis of Muc2-containing mucin granules from colonic GCs triggered by DSS exposure.

TRIM34 controls bacterial TLR ligand-triggered compound exocytosis of Muc2 from GCs

Because TRIM34-mediated Muc2 secretion occurred only upon DSS challenge, we speculated that this process was dependent on GC exposure to the commensal bacteria or their components. To test this speculation, we first used a cocktail of antibiotics (Abx) to deplete intestinal commensal bacteria. Following the depletion of the commensal bacteria, the difference in the thickness of the inner mucus layer, which had been stained by AB/PAS, between the wild-type and TRIM34-deficient mice was abolished (Fig. 5a). This observation was confirmed by the detection of Muc2 immunofluorescence staining in the mucosal layer (Fig. 5b) and the detection of mucin-containing GCs in the theca (Fig. 5c). In

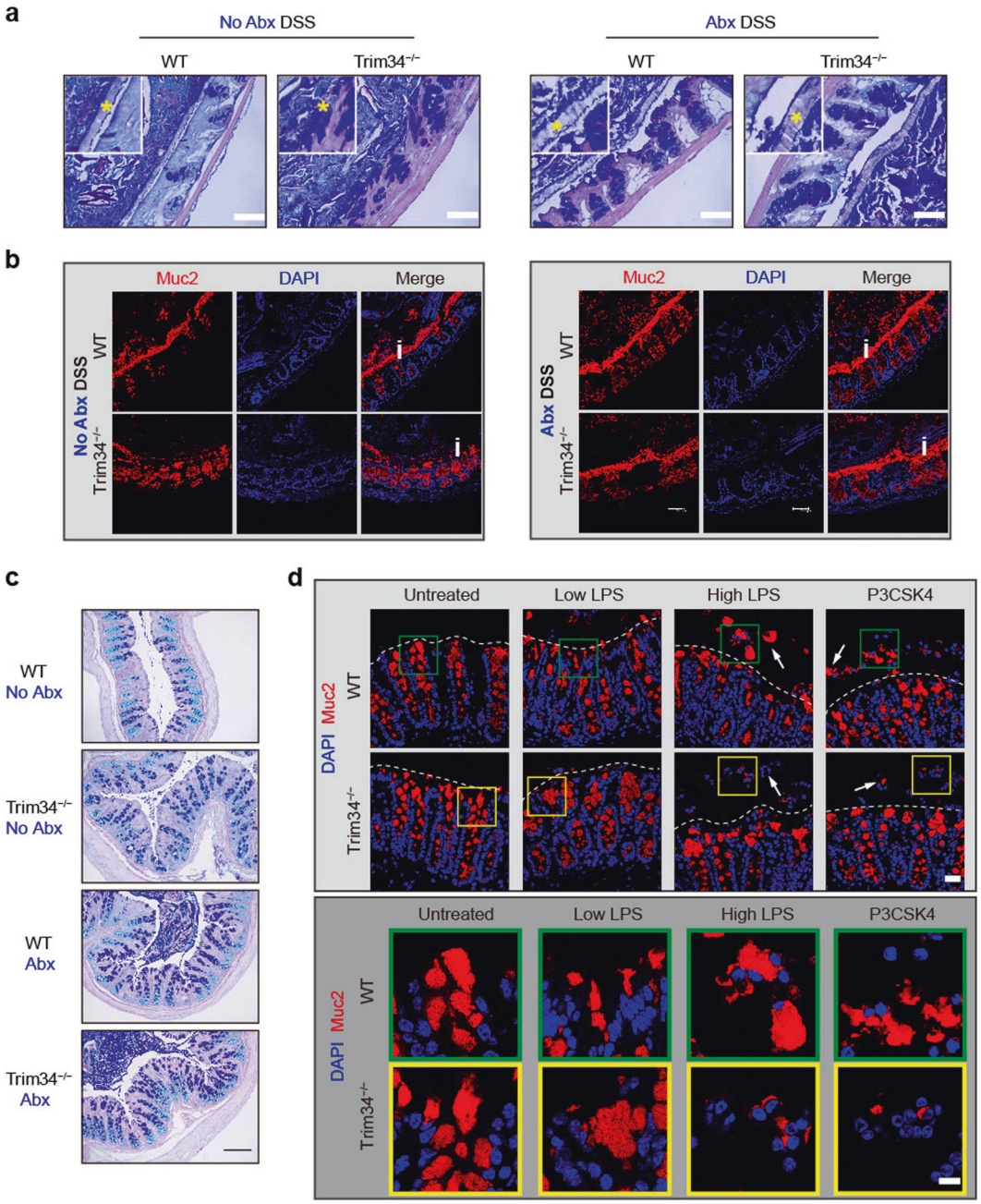

Fig. 5 TRIM34 is critical for the commensal bacterial TLR ligand-induced compound exocytosis of Muc2 from GCs. **a**–**c** Wild-type and TRIM34-deficient mice were treated with a cocktail of antibiotics for more than 2 weeks to deplete gut commensal bacteria and then challenged with or without 3% DSS for 4 days. Mice not treated with Abx were used as controls; $N = 5$ per group. **a** Representative images of AB/PAS-stained colonic sections. Scale bar, 50 μm. Asterisks highlight the inner mucus layers. **b** Colonic sections stained for Muc2 (red) and nuclei (DAPI, blue). Scale bar, 50 μm. The letter i highlights the inner mucus layer. **c** AB/PAS staining of colonic sections (no feces). Scale bar, 50 μm. **d** Freshly isolated colonic explants were unstimulated or stimulated with a low or high concentration of LPS or P3CSK4 for 45 min and then stained for Muc2 (red) and nuclei (DAPI, blue). Scale bar, 25 μm (upper). Scale bar, 10 μm (lower), magnifications from the pictures above. Arrowheads highlight Muc2 granules in crypts. Discontinuous white lines highlight the edges of crypts. The data shown represent three independent experiments

addition, the colitis severity was comparable between the TRIM34-deficient and wild-type mice that were pretreated with Abx (Supplementary Fig. 8). Clearly, we showed that the TRIM34-deficient mice display more severe defects than the wild-type mice in the integrity of the inner mucus layer, the integrity of the mucus layer and the exocytosis of mucins upon DSS treatment if mice are not pretreated with antibiotics, whereas no differences could be detected after the microbiota was depleted by Abx pretreatment (Fig. 5a–c). These results indicate that TRIM34 regulates the integrity of the inner mucus layer by controlling Muc2 exocytosis in GCs, which depends on bacterial involvement.

Bacterial TLR ligands, such as LPS, lipoprotein and flagellin, can directly stimulate GCs to release Muc2.[40] Hence, we treated colonic explants with LPS or Pam3CSK4 (a synthetic triacylated lipoprotein) in vitro, and the tissues were then stained for Muc2. As expected, we observed significant exocytosis of Muc2 in the wild-type colon explants following LPS or P3CSK4 treatment (Fig. 5d). In contrast, under the same experimental conditions, in the TRIM34-deficient mice, large Muc2 compounds were clearly detained in the crypts, and fewer secreted Muc2 compounds were detected outside the crypts (Fig. 5d). These results indicate that Muc2 secretion from GCs is tightly regulated by TRIM34 following bacterial stimulation.

TRIM34 regulates Muc2 exocytosis by modulating the TLR signaling-induced synthesis of ROS

We further explored the mechanisms by which TRIM34 regulated this exocytosis process. ROS play a central role in triggering Muc2 exocytosis from GCs.[40,28] We, therefore, assessed whether TRIM34 regulates bacterial TLR ligand-induced ROS synthesis. Colonic epithelial cells were isolated and stimulated using TLR ligands, and ROS synthesis was then measured. We found that there was a significant reduction in LPS- and P3CSK4-induced ROS synthesis in the TRIM34-deficient epithelial cells but not in the untreated cells (Fig. 6a, b). Since TLR signaling-induced both Nox/Duox-dependent ROS synthesis and mitochondrial ROS synthesis,[45,46] we used flow cytometry to measure total cellular ROS using DCFDA and mitochondrial-specific ROS using MitoSOX dye. TRIM34 deficiency reduced only the LPS-induced total cellular ROS levels but not the mitochondrial ROS levels (Fig. 6c), suggesting that TRIM34 specifically modulates the Nox/Duox-mediated ROS synthesis that is triggered by TLR signaling. To validate whether the impaired ROS synthesis accounts for the failure of Muc2 exocytosis observed in the TRIM34-deficient GCs, we used a ROS donor to attempt to rescue the function. Remarkably, an exogenous ROS donor effectively rescued the defect in exocytosis in a dose-dependent manner (Fig. 6d). These results indicate that TRIM34 controls

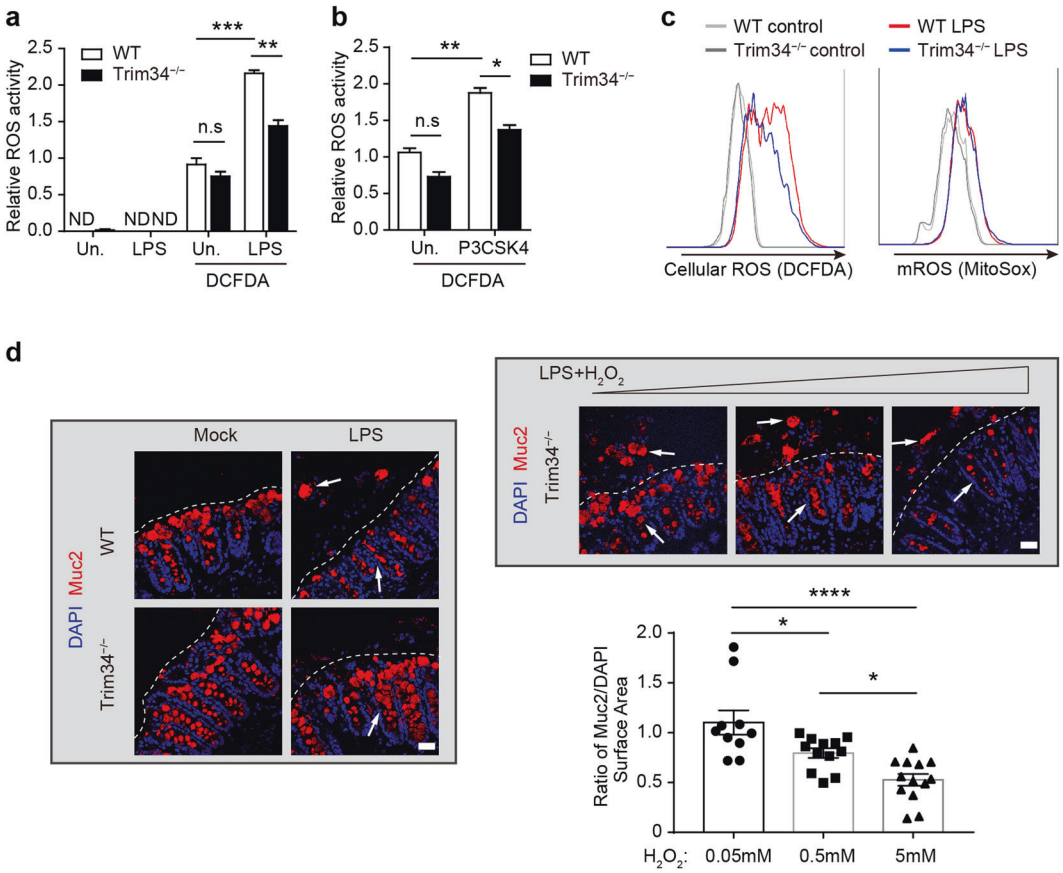

Fig. 6 TRIM34 controls Muc2 exocytosis by promoting the TLR-induced synthesis of ROS. **a**, **b** Relative ROS activity was detected using DCFDA staining in ex vivo colonic epithelial cells that were treated with LPS (**a**) or P3CSK4 (**b**). **c** Bone marrow-derived macrophages were stimulated with LPS (1 μg/ml), and ROS synthesis was then examined with flow cytometry. Total cellular ROS levels were determined using DCFDA (5 μM), and mitochondrial ROS levels were determined using MitoSOX (5 μM). **d** TRIM34-deficient colonic explants were treated with exogenous H_2O_2 (50 nM, 500 nM, or 5 μM) during LPS stimulation and then stained for Muc2 (red) and nuclei (DAPI, blue). Quantification of surface area (μm^2) based on the surface-markers for Muc2 and DAPI fluorescence using Imaris software with separate samples. The calculation of the ratio of Muc2/DAPI from different sections is shown. Arrowheads highlight either Muc2 granules in or out of crypts. Discontinuous white lines highlight the edges of crypts. The data shown represent three independent experiments and indicate the means ± SEM; $^*P < 0.05$, $^{**}P < 0.01$, $^{***}P < 0.001$, and $^{****}P < 0.0001$; ND not detected, n.s. not significant. **a**, **b**, **d** One-way ANOVA (Tukey's multiple-comparisons test)

bacterial TLR ligand-induced Muc2 exocytosis by promoting TLR-driven Nox/Duox-dependent ROS synthesis.

Members of the Nox/Duox family of NADPH oxidases are the primary regulators of ROS production in mice and humans.[47–49] There are six members of the Nox/Duox enzyme family in mice: Nox1–4, Duox1, and Duox2.[50] We examined the expression level of several members in colonic epithelial cells (Supplementary Fig. 9). Interestingly, we observed that there was a significant reduction ($P < 0.001$) in Nox1 expression in the TRIM34-deficient mice compared to the wild-type controls, which was found only under DSS-treated conditions but not in cells in the steady state, suggesting a positive correlation with the specific regulation of TRIM34 upon DSS treatment. In contrast, other Nox/Duox family members, including Nox2, Nox4, and Duox1, were not expressed significantly differently in the two groups, regardless of DSS treatment. Nox1 was originally identified and highly expressed in the colon, where it was specifically found in epithelial cells.[50] Collectively, these data suggest that TRIM34 may regulate ROS synthesis by specifically maintaining Nox1 expression levels to promote Muc2 exocytosis upon TLR ligand stimulation.

TRIM34 attenuates tumorigenesis during inflammation-driven colorectal cancer

The dysfunction of Muc2 secretion and degradation of the inner mucus layer render the host susceptible to colorectal tumorigenesis.[24] Hence, it was important to investigate whether TRIM34 deficiency leads to more severe CAC. Wild-type and TRIM34-deficient mice were injected intraperitoneally with AOM and then administered three rounds of DSS (Fig. 7a). Strikingly, the TRIM34-deficient mice lost more body weight than did the wild-type mice following every round of DSS treatment (Fig. 7b), suggesting a role for TRIM34 in recurring colitis outcomes. Fifty-seven days post AOM injection, the development of colon tumors was evaluated. We observed that TRIM34-deficient mice developed larger numbers of colon tumors and had higher tumor loads and larger tumor sizes than were observed in the control mice (Fig. 7c–f). Of

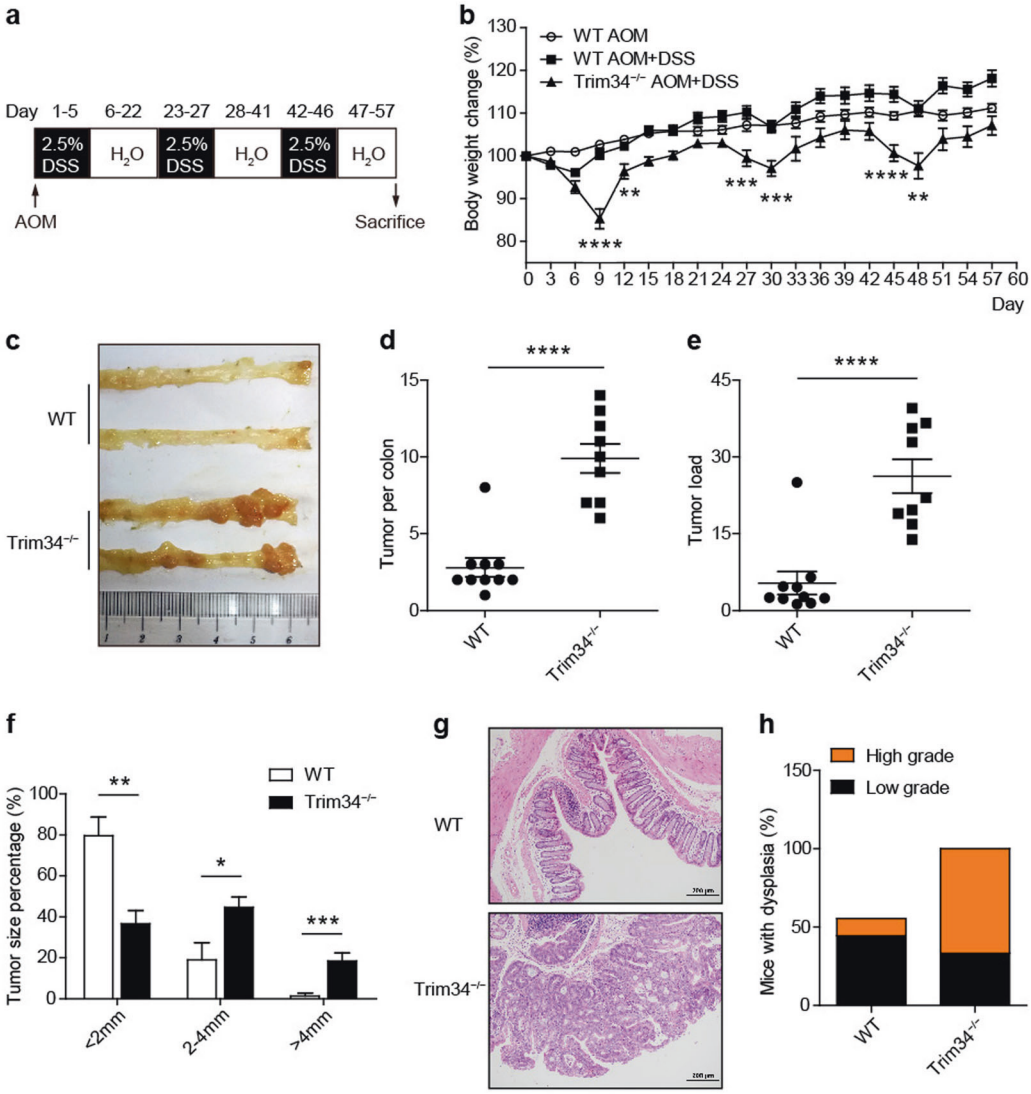

Fig. 7 TRIM34 deficiency renders mice more susceptible to colitis-associated colorectal cancer. Wild-type ($n = 10$) and TRIM34-deficient ($n = 10$) mice were treated with AOM and 3 cycles of 2.5% DSS to induce inflammation-driven colorectal cancer. Wild-type mice treated only with AOM were used as controls ($n = 5$). **a** Flow chart of the induction procedure. **b** Body weight changes were monitored every three days. **c** Representative photos of the colons. **d** Number of tumors in the colon per mouse. **e** The sum of the tumor diameters in the colon of each mouse. **f** The percentage of tumors by different diameter. **g** Representative H&E-stained colon sections. **h** Percentages of mice with dysplasia 57 days after AOM injection. Each symbol represents one mouse (**d**, **e**). The data shown are representative of two independent experiments and depict the means ± SEM; $^{*}P < 0.05$, $^{**}P < 0.01$, $^{***}P < 0.001$, and $^{****}P < 0.0001$. **b**, **d**, **e**, **f** Unpaired Student's *t* test

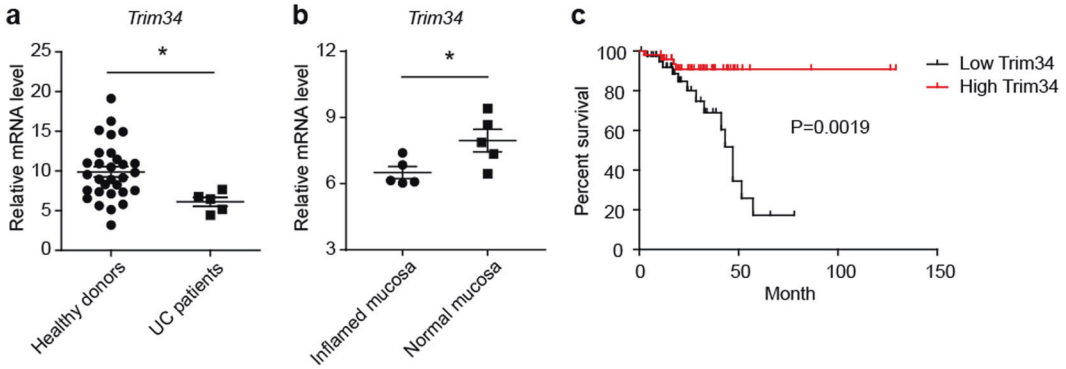

Fig. 8 Colonic TRIM34 expression is correlated with UC and rectal cancer in the clinic. **a** Relative TRIM34 mRNA abundance was determined using qPCR with colonic mucosal samples obtained from healthy donors and patients diagnosed with UC. **b** The relative abundance of TRIM34 mRNA in inflamed and normal mucosae in active UC patients. **c** Overall survival in rectal adenocarcinoma patients ($n = 92$) based on data stratified by the median normalized amount of TRIM34 mRNA in tumors according to the Colorectal Adenocarcinoma (TCGA, Provisional) data set, which includes tumor RNA-seq data and clinical correlates. *$P < 0.05$. **a** Unpaired Student's *t* test. **b** Paired Student's *t* test. **c** Log-rank test

note, the sizes of most of the tumors in the TRIM34-deficient mice were larger than 2 mm, whereas those in wild-type controls were smaller than 2 mm (Fig. 7f). Furthermore, histopathological analysis revealed that the levels of dysplasia were markedly higher in the TRIM34-deficient mice than in wild-type mice (Fig. 7g, h). Overall, these results suggest that TRIM34 plays an important role in protecting against CAC tumorigenesis.

TRIM34 abundance in the colonic mucosa is correlated with the risk of pathogenesis in UC and rectal cancer patients

As TRIM34 deficiency resulted in severe colitis and CAC in a mouse model, we next asked whether TRIM34 is clinically relevant to human UC and colorectal cancer. We first sought to determine its relevance in UC. Colonic mucosal samples were obtained from UC patients and healthy donors. We found that TRIM34 was expressed at significantly lower levels in UC patients than in healthy controls (Fig. 8a). To further explore this finding, both inflamed and normal mucosae were collected from identical individuals who were diagnosed with active UC. Interestingly, the TRIM34 expression levels were much lower in the inflamed mucosae than in the normal mucosae (Fig. 8b). Next, we sought to determine whether TRIM34 expression is correlated with colorectal cancer by using the Cancer Genome Atlas (TCGA) colorectal cancer RNA-seq data set. Patient data were stratified into two distinct groups based on median TRIM34 mRNA levels. Remarkably, a high level of TRIM34 was highly associated with increased overall survival in rectal adenocarcinoma patients (Fig. 8c). Taken together, these findings suggest that TRIM34 levels are correlated with the outcome of UC and the prognosis of rectal adenocarcinoma.

DISCUSSION

Our study demonstrates that TRIM34 plays an essential role in sustaining the integrity of the inner mucus layer in the colon by controlling Muc2 exocytosis from GCs in response to bacterial stimulation, protecting mice from severe colon inflammation. Inflammation contributes to cancer development. IBD is a predisposing factor of colorectal carcinoma, which is a leading cause of cancer-related death. In the DSS-induced mouse model, we also found that TRIM34 deficiency leads to increased susceptibility to colitis and colitis-associated tumorigenesis.

Microbial infection is frequently associated with colitis and colorectal cancer. In mouse models of colitis, inflammation development is dependent on the microbiota. In human UC, a great deal of evidence suggests that UC is caused by the inappropriate recognition of penetrating commensal bacteria.[16,17] In addition, commensal or pathogenic microbial elements have been linked to cancer development.[15] The inner mucus layer devoid of microbes plays a crucial role in preventing inappropriate sensing of the microbiota and defending against invasive pathogens. Mice lacking Muc2 have no mucus, causing the animals to spontaneously develop colitis and tumors.[23,24] Hence, maintaining an intact inner mucosal layer seems critical to decreasing the risk of colitis and colorectal cancer. However, the mechanism by which the integrity of the inner mucus layer is maintained by the host, particularly when challenged with microorganism penetration, is poorly understood. Here, we discovered that TRIM34 promotes the formation of the inner mucus layer only under conditions of bacterial involvement. Dysfunction of the mucus barrier is observed in IBD and colorectal cancer patients. For instance, the inner mucus layer in patients with active UC is thinner and penetrable to bacteria.[25] Colorectal cancers are associated with impaired mucin production and a diminished mucus barrier.[51] In our study, we revealed the clinical correlation of TRIM34 expression with the outcome of UC patients and the prognosis of rectal cancer patients. Thus, TRIM34 is suggested to be a regulator of colon inflammation and tumorigenesis in humans, as well as in mice.

TRIM family members regulate the host defense against microorganism infection. On the one hand, TRIM family members directly regulate multiple innate signaling pathways that are elicited by microbes to induce the host defense. For instance, TRIM30α negatively regulates bacterial ligand-induced TLR signaling by targeting the TAK1 complex for degradation.[32] TRIM25 promotes RIG-I signaling via direct ubiquitination to defend against RNA viruses.[52] On the other hand, TRIM family members can also be targeted by or can target microbial elements to modulate the host defense. For example, TRIM5 restricts the entry of HIV by binding to its retroviral capsid,[53] and the *Salmonella* effector protein SopA targets TRIM56 and TRIM65 to modulate innate immune responses.[54] However, nearly all studies of TRIM family-related processes in host defense have been restricted to their effects on immune responses induced by invading pathogens. In this study, we found that TRIM34 controls Muc2 secretion from GCs in response to bacterial TLR ligand stimulation, thereby promoting the integrity of the inner mucus layer to attenuate colon inflammation. This study is the first to reveal the function of TRIM family members in host defense initiated by GCs and innate immune cells. Given that the inner mucus layer is a critical defense barrier against both commensal microbes and invading pathogens, it is reasonable to conclude that TRIM34 could also protect the host from pathogen infection in the colon as it did against DSS-induced colon inflammation.

The precise mechanism by which TRIM34 maintains Nox1 expression and ROS synthesis at the molecular level is still not completely clarified in this study. Nox1 is a dominant member of NADPH oxidases in the colon epithelium, but Nox1 expression is not well understood. Since the extent of Nox-driven ROS formation is highly dependent on the level of its expression,[55] it is important to clarify the transcriptional regulation of Nox1. The expression of Nox1 has been reported to be regulated by a wide spectrum of transcription factors, including nuclear factor kB (NF-kB), activator protein 1 (AP-1), and members of the signal transducer and activator of transcription and CCAAT-enhancer binding protein (C/EBP) families; molecules influencing mRNA stability; various epigenetic processes, such as methylation and posttranslational modification of histones; and noncoding RNAs.[56,57] Many members of the TRIM family have been reported to regulate the NF-kB and/or AP-1 activity in a manner dependent on E3 ligase activity[58,30] Thus, it will be interesting to learn whether TRIM34 modulates Nox1 expression by regulating NF-kB and/or AP-1 transcription factors.

In conclusion, in the present study, we provide the first evidence demonstrating the importance of TRIM34 in maintaining a protective inner mucus layer and preventing severe colon inflammation and tumorigenesis. This information increases our understanding of the pathogenesis of colitis and inflammatory colorectal cancer. The clinical correlation of TRIM34 with UC and rectal cancer has potential application in the clinic.

ACKNOWLEDGEMENTS

We thank Dangsheng Li for critical suggestions. We are grateful to Guomei Lin for breeding the animals and Li Li for animal management. We also acknowledge the individuals involved in technical support at the Core Facility for Cell Biology and the Animal Core Facility. This work was supported by grants from the National Key Research and Development Program of China (2018YFA0507402), the National Natural Science Foundation of China (31230024), the Chinese Academy of Sciences (XDB19000000), and the National Natural Science Foundation of China (81761128009 and 81630016).

AUTHOR CONTRIBUTIONS

Q.L., Q.Y., S.Y., and C.Y. designed and performed the experiments and analyzed the data. Y.Z. and X.L. contributed to sample and reagent preparation and discussed the project. W.Z. collected the clinical samples. W.G. assisted with the intravenous injections and reagents. X.Z. and W.F. provided suggestions and reagents and discussed the data. L.M. prepared cell lines and provided reagents. Q.L. wrote the paper. B.S., J.L., J.L., and Y.Z. supervised the project and revised the paper.

ADDITIONAL INFORMATION

The online version of this article (https://doi.org/10.1038/s41423-020-0366-2) contains supplementary material.

Competing interests: The authors declare no competing interests.

REFERENCES

1. Medzhitov, R. Origin and physiological roles of inflammation. *Nature* **454**, 428–435 (2008).
2. Danese, S. & Fiocchi, C. Ulcerative Colitis. *N. Engl. J. Med.* **365**, 1713–1725 (2011).
3. Ng, S. C. et al. Early course of inflammatory bowel disease in a population-based inception cohort study from 8 countries in Asia and Australia. *Gastroenterology* **150**, 86–95 (2016).
4. Molodecky, N. A. et al. Increasing incidence and prevalence of the inflammatory bowel diseases with time, based on systematic review. *Gastroenterology* **142**, 46–54 (2012).
5. Ng, S. C. et al. Incidence and phenotype of inflammatory bowel disease based on results from the Asia-pacific Crohn's and colitis epidemiology study. *Gastroenterology* **145**, 158–165 (2013).
6. Cohen, R. D. The pharmacoeconomics of biologic therapy for IBD. *Nat. Rev. Gastroenterol. Hepatol.* **7**, 103–109 (2010).
7. de Silva, S., Devlin, S. & Panaccione, R. Optimizing the safety of biologic therapy for IBD. *Nat. Rev. Gastroenterol. Hepatol.* **7**, 93–101 (2010).
8. Grivennikov, S. I., Greten, F. R. & Karin, M. Immunity, inflammation, and cancer. *Cell* **140**, 883–899 (2010).
9. Eaden, J. A., Abrams, K. R. & Mayberry, J. F. The risk of colorectal cancer in ulcerative colitis: a meta-analysis. *Gut* **48**, 526–535 (2001).
10. von Roon, A. C. et al. The risk of cancer in patients with Crohn's disease. *Dis. Colon Rectum* **50**, 839–855 (2007).
11. Beaugerie, L. & Itzkowitz, S. H. Cancers complicating inflammatory bowel disease. *N. Engl. J. Med.* **372**, 1441–1452 (2015).
12. Weir, H. K. et al. Annual report to the nation on the status of cancer, 1975–2000, featuring the uses of surveillance data for cancer prevention and control. *J. Natl Cancer Inst.* **95**, 1276–1299 (2003).
13. Abraham, C. & Cho, J. H. Inflammatory bowel disease. *N. Engl. J. Med.* **361**, 2066–2078 (2009).
14. Saleh, M. & Elson, C. O. Experimental inflammatory bowel disease: insights into the host-microbiota dialog. *Immunity* **34**, 293–302 (2011).
15. Elinav, E. et al. Inflammation-induced cancer: crosstalk between tumours, immune cells and microorganisms. *Nat. Rev. Cancer* **13**, 759–771 (2013).
16. Campieri, M. & Gionchetti, P. Bacteria as the cause of ulcerative colitis. *Gut* **48**, 132–135 (2001).
17. Sasaki, M. & Klapproth, J. M. The role of bacteria in the pathogenesis of ulcerative colitis. *J. Signal Transduct.* **2012**, 704953 (2012).
18. Johansson, M. E. V. & Hansson, G. C. Immunological aspects of intestinal mucus and mucins. *Nat. Rev. Immunol.* **16**, 639–649 (2016).
19. Kamada, N., Seo, S. U., Chen, G. Y. & Nunez, G. Role of the gut microbiota in immunity and inflammatory disease. *Nat. Rev. Immunol.* **13**, 321–335 (2013).
20. Johansson, M. E. et al. The inner of the two Muc2 mucin-dependent mucus layers in colon is devoid of bacteria. *Proc. Natl Acad. Sci. USA* **105**, 15064–15069 (2008).
21. Johansson, M. E., Sjovall, H. & Hansson, G. C. The gastrointestinal mucus system in health and disease. *Nat. Rev. Gastroenterol. Hepatol.* **10**, 352–361 (2013).
22. Birchenough, G. M., Johansson, M. E., Gustafsson, J. K., Bergstrom, J. H. & Hansson, G. C. New developments in goblet cell mucus secretion and function. *Mucosal Immunol.* **8**, 712–719 (2015).
23. Van der Sluis, M. et al. Muc2-deficient mice spontaneously develop colitis, indicating that MUC2 is critical for colonic protection. *Gastroenterology* **131**, 117–129 (2006).
24. Velcich, A. et al. Colorectal cancer in mice genetically deficient in the mucin Muc2. *Science* **295**, 1726–1729 (2002).
25. Johansson, M. E. V. et al. Bacteria penetrate the normally impenetrable inner colon mucus layer in both murine colitis models and patients with ulcerative colitis. *Gut* **63**, 281–291 (2014).
26. Kim, J. & Khan, W. Goblet cells and mucins: role in innate defense in enteric infections. *Pathogens* **2**, 55–70 (2013).
27. McCauley, H. A. & Guasch, G. Three cheers for the goblet cell: maintaining homeostasis in mucosal epithelia. *Trends Mol. Med.* **21**, 492–503 (2015).
28. Patel, K. K. et al. Autophagy proteins control goblet cell function by potentiating reactive oxygen species production. *EMBO J.* **32**, 3130–3144 (2013).
29. Wlodarska, M. et al. NLRP6 inflammasome orchestrates the colonic host-microbial interface by regulating goblet cell mucus secretion. *Cell* **156**, 1045–1059 (2014).
30. Ozato, K., Shin, D. M., Chang, T. H. & Morse, H. C. 3rd. TRIM family proteins and their emerging roles in innate immunity. *Nat. Rev. Immunol.* **8**, 849–860 (2008).
31. Kawai, T. & Akira, S. Regulation of innate immune signalling pathways by the tripartite motif (TRIM) family proteins. *EMBO Mol. Med.* **3**, 513–527 (2011).
32. Shi, M. et al. TRIM30 alpha negatively regulates TLR-mediated NF-kappa B activation by targeting TAB2 and TAB3 for degradation. *Nat. Immunol.* **9**, 369–377 (2008).
33. Wang, Y. et al. TRIM30alpha is a negative-feedback regulator of the intracellular DNA and DNA virus-triggered response by targeting STING. *PLoS Pathog.* **11**, e1005012 (2015).
34. Yang, B. et al. Novel function of Trim44 promotes an antiviral response by stabilizing VISA. *J. Immunol.* **190**, 3613–3619 (2013).
35. Wang, Y. et al. TRIM35 negatively regulates TLR7- and TLR9-mediated type I interferon production by targeting IRF7. *FEBS Lett.* **589**, 1322–1330 (2015).
36. Wirtz, S., Neufert, C., Weigmann, B. & Neurath, M. F. Chemically induced mouse models of intestinal inflammation. *Nat. Protoc.* **2**, 541–546 (2007).
37. Neufert, C., Becker, C. & Neurath, M. F. An inducible mouse model of colon carcinogenesis for the analysis of sporadic and inflammation-driven tumor progression. *Nat. Protoc.* **2**, 1998–2004 (2007).
38. Ostanin, D. V. et al. T cell transfer model of chronic colitis: concepts, considerations, and tricks of the trade. *Am. J. Physiol. Gastrointest. Liver Physiol.* **296**, G135–G146 (2009).
39. Zaki, M. H. et al. The NOD-like receptor NLRP12 attenuates colon inflammation and tumorigenesis. *Cancer Cell* **20**, 649–660 (2011).

40. Birchenough, G. M. H., Nyström, E. E. L., Johansson, M. E. V. & Hansson, G. C. A sentinel goblet cell guards the colonic crypt by triggering Nlrp6-dependent Muc2 secretion. *Science* **352**, 1535–1542 (2016).
41. Strugala, V., Allen, A., Dettmar, P. W. & Pearson, J. P. Colonic mucin: methods of measuring mucus thickness. *Proc. Nutr. Soc.* **62**, 237–243 (2007).
42. Lian, Q. et al. Chemotherapy-induced intestinal inflammatory responses are mediated by exosome secretion of double-strand DNA via AIM2 inflammasome activation. *Cell Res.* **27**, 784–800 (2017).
43. Simmons, A. J. et al. Cytometry-based single-cell analysis of intact epithelial signaling reveals MAPK activation divergent from TNF-alpha-induced apoptosis in vivo. *Mol. Syst. Biol.* **11**, 835 (2015).
44. Wang, F. et al. Isolation and characterization of intestinal stem cells based on surface marker combinations and colony-formation assay. *Gastroenterology* **145**, 383–395.e381–321 (2013).
45. Bauernfeind, F. et al. Cutting edge: reactive oxygen species inhibitors block priming, but not activation, of the NLRP3 inflammasome. *J. Immunol.* **187**, 613–617 (2011).
46. West, A. P. et al. TLR signalling augments macrophage bactericidal activity through mitochondrial ROS. *Nature* **472**, 476–480 (2011).
47. Bedard, K. & Krause, K. H. The NOX family of ROS-generating NADPH oxidases: physiology and pathophysiology. *Physiol. Rev.* **87**, 245–313 (2007).
48. Geiszt, M. & Leto, T. L. The Nox family of NAD(P)H oxidases: host defense and beyond. *J. Biol. Chem.* **279**, 51715–51718 (2004).
49. Lambeth, J. D. & Neish, A. S. Nox enzymes and new thinking on reactive oxygen: a double-edged sword revisited. *Annu. Rev. Pathol.* **9**, 119–145 (2014).
50. Sirokmány, G., Donkó, Á. & Geiszt, M. Nox/Duox family of NADPH oxidases: lessons from knockout mouse models. *Trends Pharmacol. Sci.* **37**, 318–327 (2016).
51. Grivennikov, S. I. et al. Adenoma-linked barrier defects and microbial products drive IL-23/IL-17-mediated tumour growth. *Nature* **491**, 254–258 (2012).
52. Gack, M. U. et al. TRIM25 RING-finger E3 ubiquitin ligase is essential for RIG-I-mediated antiviral activity. *Nature* **446**, 916–920 (2007).
53. Stremlau, M. et al. The cytoplasmic body component TRIM5[alpha] restricts HIV-1 infection in Old World monkeys. *Nature* **427**, 848–853 (2004).
54. Kamanova, J., Sun, H., Lara-Tejero, M. & Galán, J. E. The salmonella effector protein SopA modulates innate immune responses by targeting TRIM E3 ligase family members. *PLoS Pathog.* **12**, e1005552 (2016).
55. Sorescu, D. et al. Superoxide production and expression of nox family proteins in human atherosclerosis. *Circulation* **105**, 1429–1435 (2002).
56. Hassler, M. R. & Egger, G. Epigenomics of cancer—emerging new concepts. *Biochimie* **94**, 2219–2230 (2012).
57. Manea, S.-A., Constantin, A., Manda, G., Sasson, S. & Manea, A. Regulation of Nox enzymes expression in vascular pathophysiology: focusing on transcription factors and epigenetic mechanisms. *Redox Biol.* **5**, 358–366 (2015).
58. Uchil, P. D. et al. TRIM protein-mediated regulation of inflammatory and innate immune signaling and its association with antiretroviral activity. *J. Virol.* **87**, 257–272 (2013).